

low. For electric field measurements, electrically short dipole antennas with a high input impedance load, such as a field effect transistor (FET) and a high-frequency diode detector, are discussed. Since the input impedance of an electrically short dipole antenna is predominantly a capacitive reactance, very broadband frequency responses can be achieved with a high impedance capacitive load. However, because conventional dipole antennas support a standing wave current distribution, the useful frequency range of these dipole antennas is usually limited by their natural resonant frequencies. In order to suppress these resonances, a resistively loaded dipole antenna has been developed. To obtain a standard antenna with increased sensitivity at a specific frequency, a half-wave tuned dipole antenna with a diode is used, to measure the induced open circuit voltage. Also used was a tuned receiver with a half-wave tuned dipole antenna, to further improve antenna sensitivity.

For magnetic field measurements, this article discusses an electrically small, resistively loaded loop antenna to achieve a broadband response. Resistive loading is achieved either with the loading resistance at the loop terminal, or by uniform resistive loading along the loop antenna. This short-circuit current loop configuration gives a very flat frequency response over a wide frequency range.

In the region near a transmitting antenna or a scatterer, the electric and magnetic field vectors are not necessarily (spatially) orthogonal or in phase. For time-harmonic fields, the end points of the field vectors trace out polarization ellipses, and the Poynting vectors lie on the surface of a cone with its end point on an ellipse. In these cases, the electric and magnetic fields may be measured separately or, using the single-loop antenna element described in this article, they may be measured simultaneously.

Photonic sensors are also discussed; they provide the wide bandwidth and low dispersion necessary to maintain the fidelity of time-domain signals. Since they consist of electro-optic modulators and optical fibers, they are free from electromagnetic interference, and there is minimal perturbation of the field being measured.

Throughout the discussion, the interplay between measured quantities and predicted (modeled) quantities is emphasized. The ability of measurements and the restrictions imposed by rigorous theoretical analysis of given models are discussed for the frequencies from 10 kHz to 40 GHz and upward.

## ELECTROMAGNETIC FIELD MEASUREMENT

To establish standards for conducting electromagnetic (EM) field measurements, measurements must be made (1) in anechoic chambers, (2) at open area test sites, and (3) within guided-wave structures; and a means to transfer these measurements from one situation to another must be developed. The underlying principles of these measurement and transfer standards are: (1) measurements and (2) theoretical modeling. That is, a parameter or a set of parameters is measured, or a parameter is calculated by established physical and mathematical principles.

Various electromagnetic field sensors for measuring radio-frequency (RF) electric and magnetic fields are discussed be-

## ELECTRIC FIELD SENSORS

### An Electrically Short Dipole Antenna with a Capacitive Load

Most electric field sensors consist of dipole antennas. The induced open circuit voltage  $V_{oc}$  at the dipole antenna terminal is given by

$$V_{oc} = E_{inc} L_{eff} \quad (1)$$

where  $E_{inc}$  is the normal incident electric field strength and  $L_{eff}$  is the effective length of the dipole antenna. For an electrically short dipole antenna whose physical length is much shorter than the wavelength, the effective length  $L_{eff}$  and driv-

ing point capacitance  $C_a$  are approximately (1)

$$L_{\text{eff}} = \frac{L(\Omega - 1)}{4(\Omega - 2 - \ln 4)} \quad (2)$$

and

$$C_a = \frac{4\pi\epsilon_0 L}{2(\Omega - 2 - \ln 4)} \quad (3)$$

where  $L$  is the physical length of the dipole antenna,  $\epsilon_0$  is the free space permittivity,  $\Omega$  is the antenna thickness factor  $\Omega = 2 \ln(L/a)$ , and  $a$  is the antenna radius.

For an electrically short dipole antenna with a capacitive load  $C$ , the transfer function is given by (1)

$$S(f) = \frac{V_o(f)}{E_{\text{inc}}(f)} = \frac{h\kappa/2}{1 + C/C_a} \quad (4)$$

where

$$C_a = \frac{4\pi h}{c\zeta_0(\Omega - 2 - \ln 4)} \quad (5)$$

$$\kappa = \frac{\Omega - 1}{\Omega - 2 + \ln 4} \quad (6)$$

and

- $a$  = antenna radius
- $C$  = capacitance of load
- $C_a$  = capacitance of antenna
- $E_{\text{inc}}$  = incident electric field
- $h$  = half of the physical length of the dipole antenna
- $V_o$  = output voltage of the antenna
- $\zeta_0$  = free space impedance
- $c$  = speed of light in free space
- $\Omega$  = antenna thickness factor,  $\Omega = 2 \ln(2h/a)$

Since the input impedance of an electrically short dipole antenna is almost purely capacitive, it is possible to achieve a frequency independent transfer function with a capacitive load, as indicated in Eq. (4). In practice, the load impedance is seldom purely capacitive, but also may have a resistive component. This resistive component will cause a 6 dB per octave roll-off at the low end of the frequency range.

### An Electrically Short Dipole Antenna with a Diode

A common standard sensor used for EM field measurements is an electrically short dipole antenna with a diode load connected to a dc metering unit by an RF filter transmission line. The main advantage of including a diode is to make the frequency response of the sensor very flat, even at higher frequencies where an FET amplifier is not readily available. When used with a high-input impedance detector, the sensor can serve as a portable and compact transfer standard.

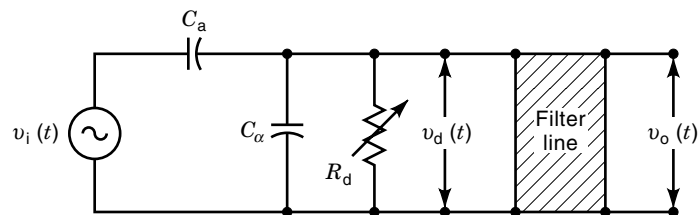


**Figure 1.** Thevenin's equivalent circuit of an electrically short dipole antenna with a shunt diode detector.

Figure 1 represents a dipole antenna, which can be used to determine the signal from the transmission line for a given incident electric field (2). This circuit is valid for the frequency range to be considered (dc and  $f > 1$  MHz). In Fig. 1, the small antenna resistance has been neglected. The stray gap capacitance of the filter line from the antenna terminal connections has been included in the effective shunt capacitance  $C_d$ . The antenna capacitance is given by  $C_a$ .

When a first-order, nonlinear differential equation associated with the Thevenin's equivalent nonlinear circuit (shown in Fig. 1) is solved for the detected dc voltage  $V_o$ , for a small induced RF voltage  $V_i$  (2)

$$V_o = -\frac{\alpha}{4} \left( \frac{V_i}{1 + C_d/C_a} \right)^2 \quad (7)$$

where  $\alpha$  ( $\approx 38 \text{ V}^{-1}$ ) is derived from the diode characteristics, while for large  $V_i$

$$V_o \cong -\frac{V_i}{1 + C_d/C_a} \quad (8)$$

Equation (7) indicates that for a small induced RF voltage  $V_i$ , the output dc voltage  $V_o$  is a square law function of the induced voltage. On the other hand, Eq. (8) indicates that, for a large induced voltage  $V_i$ , the output dc voltage  $V_o$  is directly proportional to the induced voltage.

### A Resistively Loaded Dipole Antenna with a Diode

A conventional dipole antenna essentially supports a standing wave current distribution and is, therefore, highly frequency sensitive. For the antenna to have a flat frequency response beyond any natural resonant frequency, a traveling wave dipole antenna was realized by use of continuously tapered resistive loading (3,4). If the internal impedance per unit length  $Z^i(z)$  as a function of the axial coordinate  $z$  is expressed as

$$Z^i(z) = \frac{60\Psi}{h - |z|} \quad (9)$$

then the current distribution  $I_z(z)$  along the linear antenna is that of a traveling wave

$$I_z(z) = \frac{V_i}{60\Psi(1 - j/kh)} \left[ 1 - \frac{|z|}{h} \right] e^{-jk|z|} \quad (10)$$

where  $2h$  is the dipole antenna's total physical length,  $k$  is

the wavenumber,  $V_i$  is the driving voltage, and  $\Psi$  is given by

$$\Psi = 2 \left[ \sinh^{-1} \frac{h}{a} - C(2ka, 2kh) - jS(2ka, 2kh) \right] + \frac{j}{kh} (1 - e^{-j2kh}) \quad (11)$$

where  $a$  is the radius of the dipole, and  $C(x, y)$  and  $S(x, y)$  are the generalized cosine and sine integrals. The main advantage of a resistively loaded dipole antenna with a diode is the very flat frequency response of the sensor system. A shortcoming of this sensor system is the relatively low sensitivity. To overcome this problem, a standard half-wave tuned dipole antenna should be used.

### A Tuned Half-Wave Dipole Antenna

The magnitude of the electric field component at a given point in an electromagnetic field is determined from the open circuit voltage  $V_{oc}$  induced in a standard half-wave receiving dipole antenna as obtained from Eq. (1). The induced voltage is measured across the center gap of the dipole antenna, which is oriented parallel to the electric field vector of the incident field.

The RF voltage induced in the half-wave standard dipole antenna is rectified by a high impedance Schottky barrier diode connected in shunt across the center gap of the antenna. The diode output is filtered by a balanced RC network, and this dc voltage is measured with a high impedance dc voltmeter.

The effective length  $h_e$  of a thin dipole antenna near resonance and the required total length  $L$  for resonance are given by (1)

$$h_e = \frac{\lambda}{\pi} \tan \left( \frac{\pi h}{\lambda} \right) \quad (12)$$

and

$$L = (\lambda/2) \left[ 1 - \frac{0.2257}{\ln(\lambda/D) - 1} \right] \quad (13)$$

where  $D$  is the diameter of the standard dipole antenna.

To further increase the sensitivity of a standard antenna, a half-wave tuned dipole antenna with a narrow band receiver should be used. In this case, the transfer function  $S(f)$  is given by

$$S(f) = \frac{V_L(f)}{E_{inc}(f)} = \frac{h_e Z_a}{Z_a + Z_r} \quad (14)$$

where  $V_L$  is the voltage across the receiver load,  $E_{inc}$  is the incident electric field,  $h_e$  is the effective length of the tuned dipole,  $Z_a$  is the antenna impedance, and  $Z_r$  is the receiver input impedance ( $\sim 50 \Omega$ ). The input impedance of the antenna  $Z_a$  is complicated and is given in (1). When the cable losses are significant, they should be included in  $Z_a$ .

## MAGNETIC FIELD SENSORS

### An Electrically Small Loop Antenna with a Loading Resistance

A magnetic field sensor consists of an electrically small, balanced loop antenna. The voltage  $V_i$  induced in an electrically

small loop antenna by an electromagnetic wave incident on the loop antenna is determined from Maxwell's equations and Stokes's theorem, and is given by (1)

$$V_i = \int E_i d\ell = j\omega\mu H_i NS \quad (15)$$

where  $E_i$  is the tangential electric field induced around the loop antenna,  $l$  is the circumference of the loop antenna,  $\omega$  is the angular frequency of  $E_i$ ,  $\mu$  is the permeability of the loop antenna core,  $H_i$  is the component of the magnetic field normal to the plane of the loop antenna,  $N$  is the number of loop antenna turns, and  $S$  is the area of the loop antenna. The induced voltage  $V_i$  of an electrically small loop antenna is proportional to frequency, the number of loop turns, and the area of the loop antenna.

To make the response of a loop antenna flat over the frequency range of interest, the  $Q$  of the antenna has to be reduced through a loading resistance. The resonance of a loop antenna is the result of the combined effect of the distributed capacitance of the loop antenna, the gap capacitance, and the capacitance of the amplifier along with the inductance of the loop antenna. The equivalent circuit for an electrically small loop antenna is shown in Fig. 2. Here  $V_i$  is the induced voltage,  $L$  is the loop inductance,  $C$  is the capacitance,  $R$  is the loading resistance, and  $V_o$  is the voltage across the loading resistance. Then the response of an electrically small loop antenna is given by (1)

$$\frac{V_o}{V_i} = \frac{-j \frac{1}{\delta}}{\frac{1}{Q} + j \left( \delta - \frac{1}{\delta} \right)} \quad (16)$$

where

$$Q = \frac{R}{X_0}, \quad X_0 = \omega_0 L = \frac{1}{\omega_0 C}, \quad \delta = \frac{\omega}{\omega_0}, \quad \omega_0 = \frac{1}{\sqrt{LC}} \quad (17)$$

The inductance  $L$  and the capacitance  $C$  of a loop antenna can be given by

$$L = \mu b \ln \left( \frac{b}{a} \right) \quad (18)$$

and

$$C = \frac{2\epsilon b}{\ln \left( \frac{b}{a} \right)} \quad (19)$$

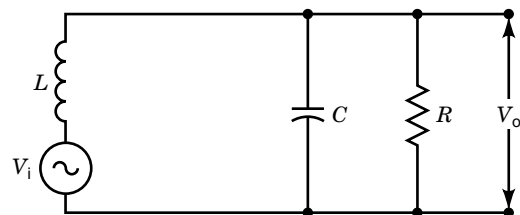


**Figure 2.** Thevenin's equivalent circuit of an electrically small loop antenna with a loading resistance.

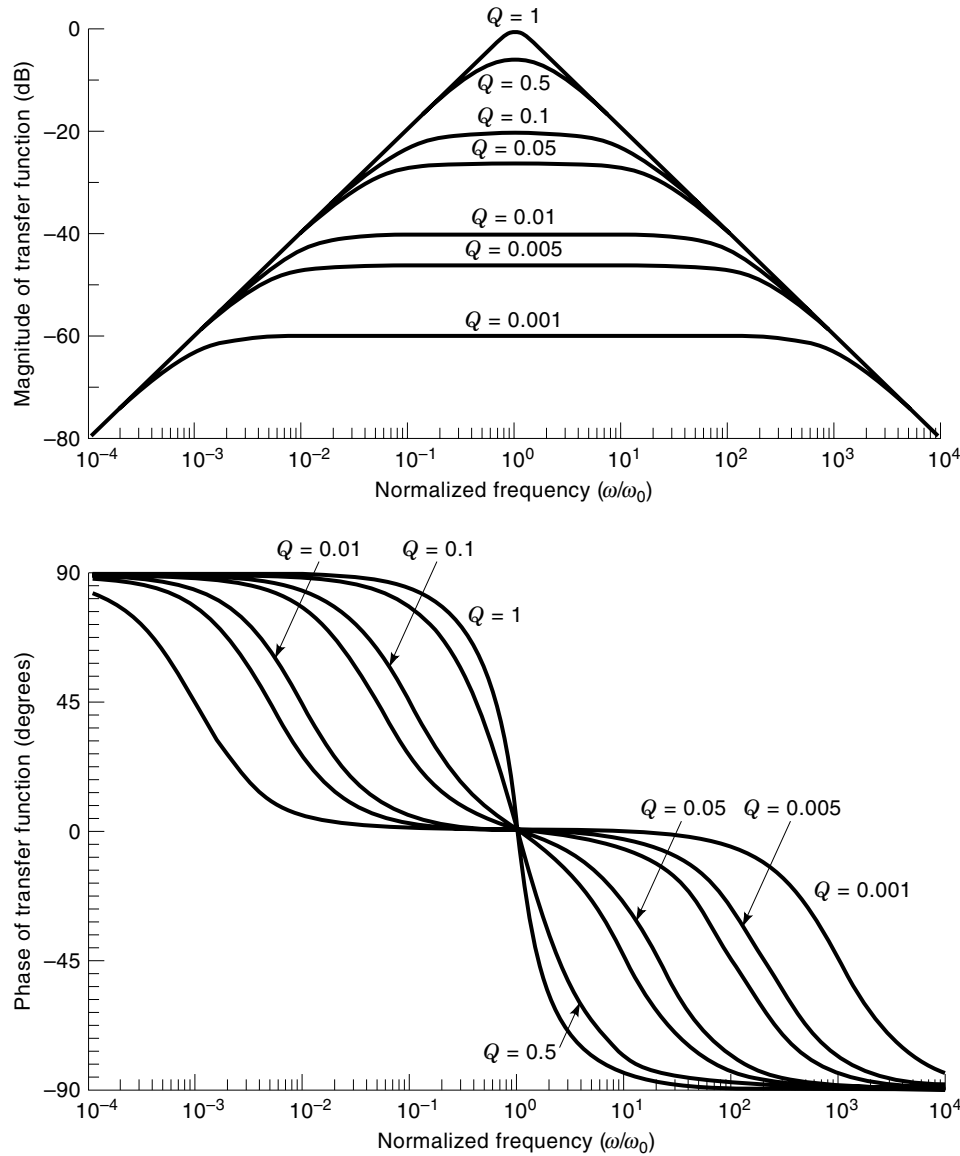


**Figure 3.** The normalized transfer function of a loop antenna as a function of normalized frequency for different value of  $Q$ .

where  $\mu$  is the permeability of the medium,  $b$  is the loop antenna radius, and  $a$  is the radius of the loop wire.

The transfer function of  $S(f)$  of an electrically small loop antenna can be obtained by combining Eqs. (15) and (16).

$$S(f) = \frac{V_o}{H_i} = \omega_o \mu N S \frac{1}{\frac{1}{Q} + j \left( \delta - \frac{1}{\delta} \right)} \quad (20)$$

The normalized transfer function  $S_n(f)$  of a loop antenna with a loading resistor is given by

$$S_n(f) = \frac{1}{\frac{1}{Q} + j \left( \delta - \frac{1}{\delta} \right)} \quad (21)$$

as a function of the normalized frequency  $\delta = \omega/\omega_o$  and is given in Fig. 3 for various  $Q < 1$ . Figure 3 shows that the upper frequency end  $\omega_h$  of the 3 dB roll-off point is given by  $\delta_h Q = 1$  and, similarly, the corresponding low frequency  $\omega_l$  of

the 3 dB roll-off point is given by  $\delta_l/Q = 1$ . Thus, from these conditions,

$$\delta_h \delta_l = \frac{\omega_h \omega_l}{\omega_o^2} = 1 \quad (22)$$

or

$$\omega_o = \sqrt{\omega_h \omega_l} \quad (23)$$

The self-resonant frequency of a loop antenna is therefore the geometrical mean of the highest and lowest cutoff frequencies.

#### AN ELECTROMAGNETIC FIELD SENSOR FOR SIMULTANEOUS ELECTRIC AND MAGNETIC FIELD MEASUREMENTS

The electric and magnetic field sensors discussed above measure either the electric or magnetic field only and, therefore, cannot measure complicated EM fields such as those with re-

active near field components and multipath reflections. For this reason, a single sensor capable of performing simultaneous electric and magnetic field measurements was developed (5,6). In this case, a loop antenna is loaded at diametrically opposite points with equal impedances. Across one load, the magnetic loop response adds to the electric dipole response, whereas across the other load, the magnetic loop response subtracts from the electric dipole response. Thus, by taking the sum and difference of currents across loads at diametrically opposite points, the magnetic loop response and electric dipole response can be separated. That is, the sum current gives a measure of the magnetic field, whereas the difference current gives a measure of the electric field.

To explain the basic characteristics of a doubly loaded loop antenna, the currents  $I_1$  and  $I_2$  at each load are given by (5)

$$I_1 = 2\pi b E_{\text{inc}} \left( \frac{f_0 Y_0}{1 + 2Y_0 Z_L} + \frac{f_1 Y_1}{1 + 2Y_1 Z_L} \right) \quad (24)$$

and

$$I_2 = 2\pi b E_{\text{inc}} \left( \frac{f_0 Y_0}{1 + 2Y_0 Z_L} - \frac{f_1 Y_1}{1 + 2Y_1 Z_L} \right) \quad (25)$$

where  $b$  is the radius of the loop,  $E_{\text{inc}}$  is the incident electric field,  $Z_L$  is the load impedance,  $Y_0$  is the admittance for the magnetic loop response, and  $Y_1$  is the admittance for the electric dipole antenna response of a loop. In general,  $Y_0$  is much larger than  $Y_1$ .  $f_0$  and  $f_1$  are Fourier coefficients of the incident wave. For a loop antenna orientation of maximum electric and magnetic field response,  $f_0 = j\beta b/2$  and  $f_1 = 1/2$ . Taking the sum and difference of these currents yields (5)

$$I_{\Sigma} = \frac{1}{2} (I_1 + I_2) = 2\pi b E_{\text{inc}} \frac{f_0 Y_0}{1 + 2Y_0 Z_L} \quad (26)$$

and

$$I_{\Delta} = \frac{1}{2} (I_1 - I_2) = 2\pi b E_{\text{inc}} \frac{f_1 Y_1}{1 + 2Y_1 Z_L} \quad (27)$$

This indicates that the sum current can be used to measure the magnetic field and the difference current can be used to measure the electric field. In general,  $2Y_0 Z_L > 1$  for the magnetic field loop antenna current. Therefore, when the antenna is oriented for maximum response,  $I_{\Sigma}$  can be approximated as

$$I_{\Sigma} \cong j \frac{E_{\text{inc}}}{2Z_L} \pi b^2 \beta \quad (28)$$

This indicates that the magnetic loop current is approximately proportional to the product of frequency and the area of the loop antenna, and is inversely proportional to the load impedance. Similarly, for the electric field dipole current, assuming that  $2Y_1 Z_L \ll 1$ ,

$$I_{\Delta} \cong \pi b E_{\text{inc}} Y_1 \quad (29)$$

which is approximately proportional to the product of the circumference of the loop antenna and frequency, since  $Y_1$  has a capacitive susceptance (positive) and increases with frequency. This device is intended not only to measure the polarization ellipses of the electric and magnetic field vectors in

the near field region, but also to measure the time-dependent Poynting vector and thus describe the energy flow.

## PHOTONIC ELECTROMAGNETIC FIELD SENSORS

Properly designed photonic EM field sensors provide the wide bandwidth and low dispersion necessary to maintain the fidelity of time-domain signals so that both amplitude and phase information can be retrieved (7). They are free from electromagnetic interference, and there is minimal perturbation of the field being measured.

A number of photonic passive sensors for EM field measurements have been reported in the literature (7). These are systems in which the sensor head contains no active electronics or power supplies. Optical measurement systems of the typical photonic EM field sensors is shown schematically in Fig. 4. Light from a laser is launched into an optical fiber link and serves as an optical signal carrier. At the sensor head, the EM field induces a voltage across the modulator crystal and changes its index of refraction. The crystal index changes occur at the frequency of the impressed EM field and result in a modulation in the amplitude of the optical carrier. At the receiver end of the fiber the light is converted to an electrical signal by a photodiode and is suitably amplified for analysis with a spectrum analyzer, oscilloscope, or other signal processor. The electro-optic interaction is weak, and, except for very high fields, the gain of a small antenna is usually required to obtain adequate modulation.

For the measurement of a pulsed electric field, an antenna with a flat broadband response is most desirable. A resistively loaded dipole antenna gives a nonresonant frequency response and is, therefore, ideal for use in the time-domain measurement of electromagnetic fields (3,4). Electro-optical modulators that are driven by antenna feeds are characterized as a function of the voltage applied to their electrodes. A convenient parameter for characterizing a modulator's performance is the voltage  $V_{\pi}$  that is needed across the electrode to drive a modulator between maximum and minimum optical power levels. In general, a modulator transfer function is nonlinear. However, in most cases of interest, the field-induced RF voltages on the modulator's electrodes are small compared to  $V_{\pi}$ , and a small signal linear transfer function evaluated at the operating bias point is appropriate. The most desirable operating bias point is where the modulator's sensitivity and linear range are at maximum. The physical characteristics of four modulators used in photonic EM field sensors are given in Table 1.

### Pockels Cell

Pockels cell modulators often are used in EM field sensors. The small signal transfer function takes the form given in Table 1, when the constant phase shift  $\Phi_0$  is set equal to  $-\pi/2$  by introducing a quarter wave retardation plate into the cell. This biases the modulator at its point of maximum sensitivity and linearity. The characteristic voltage of a bulk crystal modulator is limited by (1) the magnitude of the electro-optic coefficients for available materials, (2) the minimum dimensions of crystals that can be handled as discrete optical elements, and (3) the maximum crystal lengths acceptable for the highest desired operating frequency. For operation to 5 GHz, the lowest obtainable values for  $V_{\pi}$  are on the order of 100 V for  $\text{LiNbO}_3$ . It is relatively easy to increase  $V_{\pi}$  and re-

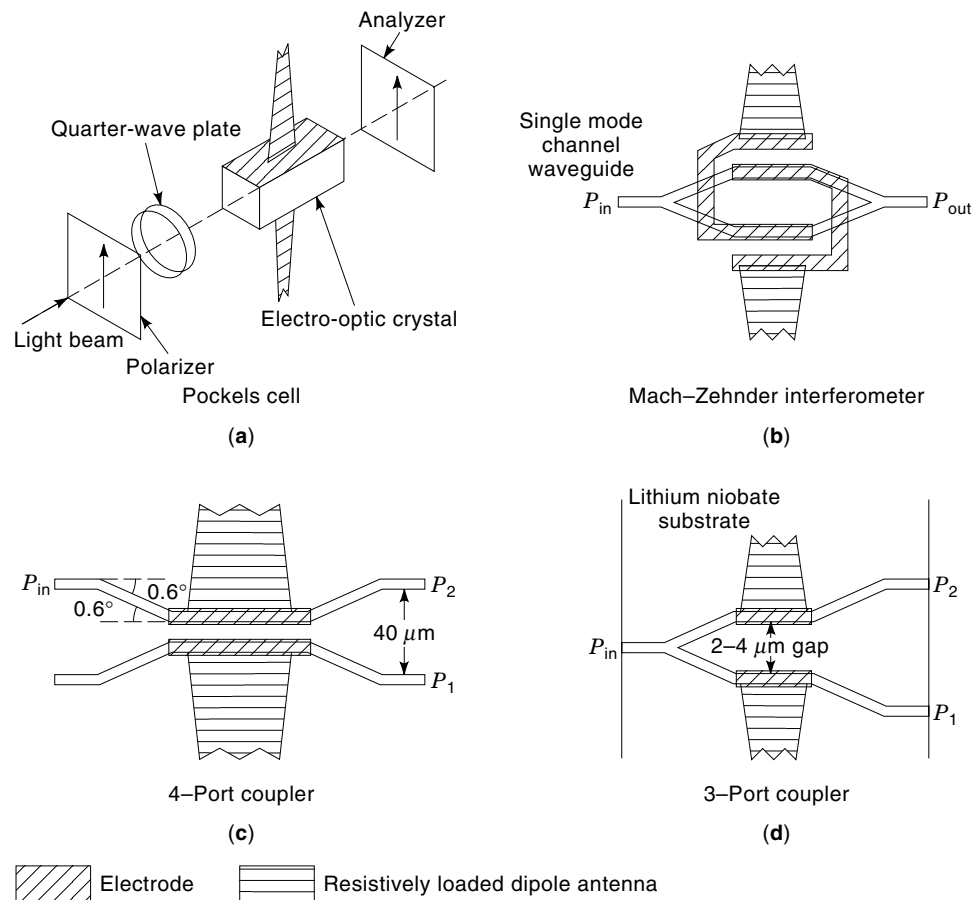


**Figure 4.** Measurement system of a photonic EM field sensor.

duce the modulator's sensitivity in order to measure high fields. In one application of this technology for measuring fields from electromagnetic pulses, a crystal of  $\text{Bi}_4\text{Ge}_3\text{O}_{12}$  (BGO), which has cubic symmetry and reduced temperature sensitivity, is used in a Pockels cell modulator and has a  $V_\pi$  of approximately 2100 V.

### Mach-Zehnder Interferometer

Modulators based on Mach-Zehnder (MZ) interferometers and fabricated using optical guided wave (OGW) technologies have found widespread use in the fiber optics communications industry. Their use as EM field sensors also has been investi-

gated (7). Photolithography is used to fabricate OGW modulators by defining the waveguide channels and then diffusing titanium into the surface of a  $\text{LiNbO}_3$  crystal along these channels. The transfer function for an MZ interferometer is identical to that of the Pockels cell. The static phase shift  $\Phi_0$  is due to differences in the optical path length in the interferometer arms. Significantly,  $V_\pi$  for this device is typically two orders of magnitude smaller than that for a Pockels cell modulator of the same material and frequency response. The higher sensitivity is typical of most OGW modulators and arises from the higher fields created in the crystal with the closely spaced electrodes that are achievable using photolithography. The principal problems to date with the MZ inter-

**Table 1. Transfer Functions for Electro-Optic Modulators**

Modulator	General	Small Signal
Pockels Cell	$\cos^2\left(\frac{\pi}{2}V_n + \frac{\phi_0}{2}\right)$	$\frac{\pi}{2V_\pi}$
Mach-Zehnder	$\cos^2\left(\frac{\pi}{2}V_n + \frac{\phi_0}{2}\right)$	$\frac{\pi}{2V_\pi}$
4-Port Coupler	$\frac{1}{1+3V_n^2} \sin^2\left(\frac{\pi}{2}\sqrt{1+3V_n^2}\right)$	$\approx \frac{1.6}{V_\pi}$
3-Port Coupler	$\frac{1}{2} - \frac{2V_n}{1+4V_n^2} \sin\left(\frac{\pi}{2\sqrt{2}}\sqrt{1+4V_n^2}\right)$	$\frac{2}{V_\pi} \sin \frac{\pi}{2\sqrt{2}} = \frac{1.79}{V_\pi}$

ferometer have been the difficulty in obtaining the correct value for  $\Phi_0$  during fabrication, and its temperature and wavelength dependence.

### Directional Coupler

Directional couplers are also OGW devices that have been investigated for use as EM field sensors (7). In the interaction region, the two waveguides lie close enough together that the evanescent field of the lightwave in one guide couples into the other guide. In such a coupled-mode system, the energy in one lightguide can be switched to the other guide by changing the relative propagation constants in the channels with the electro-optic effect. If the fabrication parameters are chosen correctly, the transfer function given in the literature (7) for the directional coupler can be written in the form given in Table 1.

## ELECTROMAGNETIC FIELD STANDARDS

### Transverse Electromagnetic Cell

Transverse electromagnetic (TEM) transmission line cells are devices used for establishing standard EM fields in a shielded environment (8). Their application is becoming increasingly widespread because of their versatility, measurement accuracy, and ease of operation.

A TEM cell is essentially a 50  $\Omega$  triplate transmission line with the sides closed in, to prevent radiation of RF energy into the environment and to provide electrical isolation. A properly designed cell, terminated in its characteristic impedance, is capable of producing a calculable electric and magnetic field for calibrating an electrically small antenna or RF sensor. The cell consists of a section of rectangular coaxial transmission line tapered at each end to adapt to standard coaxial connectors. The line and tapered transitions are designed to have a nominal characteristic impedance of 50  $\Omega$  along their length, to ensure minimum voltage standing wave ratio. A fairly uniform EM field is established between the plates inside the cell when RF energy is conducted in the line from a transmitter connected to the cell's input port. A 50  $\Omega$  termination is connected to the cell's output port. The expression for determining the electric field  $E$  in the cell is given by

$$E = \frac{V}{b} = \frac{\sqrt{PZ_0}}{b} \quad (30)$$

where  $V$  is the rms voltage on the septum (center conductor),  $b$  is the separation distance between the septum and lower or upper walls,  $P$  is the net power flow to the cell and  $Z_0$  is the real part of the cell's characteristic impedance  $\cong 50 \Omega$ .

A wave traveling through a cell has essentially the free space impedance ( $\cong 120\pi \Omega$ ), thus providing a close approximation to a far-field plane wave propagating in free space. The design of TEM cells can be based on an approximate equation for the characteristic impedance of a rectangular transmission line (8)

$$Z_0 \cong \frac{377}{4} \left\{ \left[ \frac{p}{q} - \frac{2}{\pi} \ln \left( \sinh \frac{\pi g}{2q} \right) \right] - \frac{\Delta c}{\epsilon_0} \right\}^{-1} \quad (31)$$

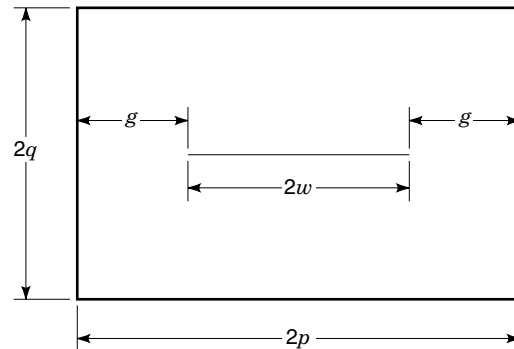


Figure 5. Cross-sectional view of a TEM cell.

where  $p$ ,  $q$ , and  $g$  are shown in Fig. 5, and  $\Delta c/\epsilon_0$  is related to the fringing capacitance between the edges of the septum and the side walls. For large gaps ( $g/p > 0.2$ ) this fringing term approaches zero (8).

The upper useful frequency for a cell is limited by distortion in the test field caused by multimoding and resonances that occur within the cell at frequencies above the cell's multimode cut off. Resonant frequencies associated with these modes can be found from the expression (8)

$$F_{\text{res}} = \sqrt{f_{mn}^2 + \left( \frac{c\ell}{2L} \right)^2} \quad (32)$$

where  $f_{mn}$  are the frequencies of the higher-order mode(s) excited inside the cell,  $c$  is the wave propagation velocity ( $\cong 3.0 \times 10^8$  m/s),  $L$  is the resonant length of the cell in meters, and  $l$ ,  $m$ , and  $n$  are integers corresponding to multiples of the resonant length and the particular waveguide mode. The influence of the first-order TE modes does not become significant until approaching their resonances. Since most cells are designed with the center plate (septum) centered symmetrically, the odd-order TE modes are not excited in an empty cell. The presence of a device placed in the cell will, however, excite these modes in varying degrees, depending on its size, shape, and placement.

### Waveguide Chamber

For the frequency range of 300 MHz to 1000 MHz, one can use a waveguide section with a rectangular cross-section with a width-to-height (aspect) ratio of two to one. The length of a guide "cell" must exceed two wavelengths over the specified frequency band, in order to create a fairly uniform field within the guide. Electromagnetic power is transmitted through the guide to a matched resistive load, and the maximum frequency is limited by the requirement that power propagates in the guide in the dominant TE<sub>10</sub> mode. In this well-known case, the direction of the electric field vector is across the narrow face of the guide.

Assuming good conductivity of the waveguide walls, an air dielectric, and sinusoidal excitation, the lowest cutoff frequency  $f_{co}$  is

$$f_{co} = \frac{c}{2a} \quad (33)$$

where  $c$  is the wave propagation velocity ( $\cong 3.0 \times 10^8$  m/s) and  $a$  is the guide width.

The longest or cutoff wavelength is given by  $\lambda_{co} = 2a$ . The wavelength  $\lambda_{wg}$  inside the guide for these operating conditions is

$$\frac{1}{\lambda_{wg}} = \sqrt{\left(\frac{1}{\lambda_0}\right)^2 - \left(\frac{1}{\lambda_{co}}\right)^2} \quad (34)$$

where  $\lambda_0$  is the free space wavelength.

The transverse impedance  $Z_w$  of the wave traveling in the guide is

$$Z_w = \frac{-E_y}{H_z} = \zeta_0 \left(\frac{\lambda_{wg}}{\lambda_0}\right) = \frac{\zeta_0}{\sqrt{1 - (\lambda_0/2a)^2}} \quad (35)$$

where  $\zeta_0$  is the intrinsic impedance of free space ( $\cong 120\pi$ ).

The direction of the electric field vector is across the narrow face of the guide, and its rms magnitude at the center of a rectangular waveguide is given by

$$E = \sqrt{\frac{2Z_w P_z}{ab}} \quad (36)$$

and, similarly, the rms magnitude of the magnetic field in the guide center is given by

$$H = \sqrt{\frac{2P_z}{Z_w ab}} \quad (37)$$

where  $P_z$  is the total power flow in the guide, and  $ab$  is the cross-sectional area of the waveguide ( $= 0.5 a^2$ ).

### Microwave Anechoic Chambers

Microwave anechoic chambers currently are used for a variety of indoor antenna measurements, electromagnetic field measurements, electromagnetic interference (EMI) measurements, and electromagnetic compatibility (EMC) measurements. The primary requirement is that a transmitting antenna at one location within a chamber or at a chamber wall generates a known field throughout a volume of the chamber, which has dimensions sufficient to perform EM field measurements. This volume is frequently called a *quiet zone*, and the level of reflected waves within it will determine the performance of the anechoic chamber.

Electromagnetic field measurements in an anechoic chamber usually are performed in the near-field region of a transmitting standard antenna. To establish the standard field, the radiated field intensity in the near-field region of the transmitting antenna is calculated. The antennas typically used for the anechoic chamber measurements consist of a series of open-ended waveguides at frequencies below 450 MHz, and a series of rectangular pyramidal horn antennas at frequencies above 450 MHz.

The electric field strength at a specific distance from the radiating antenna is calculated from measurements of the power delivered to the transmitting antenna and a knowledge of the gain of the antenna as a function of frequency and distance to the field point. The equation used to calculate the electric field  $E$  on the boresight axis of the transmitting an-

tenna is

$$E = \frac{1}{d} \sqrt{\frac{\zeta_0 P_{net} G}{4\pi}} \cong \frac{\sqrt{30 P_{net} G}}{d} \quad (38)$$

where  $P_{net}$  is the net power delivered to the transmitting antenna,  $\zeta_0$  is the free space impedance ( $\cong 120\pi \Omega$ ),  $G$  is the near-field gain of the transmitting antenna at the given frequency and distance, and  $d$  is the distance from the center of the aperture of the transmitting antenna (horn or open-ended waveguide) to the on-axis field point.

The net power  $P_{net}$  delivered to the transmitting antenna is the difference between the incident  $P_{inc}$  and reflected  $P_{refl}$  powers as measured with a calibrated directional coupler (4 ports) with calibrated power meters. In order for measurements to be accurate, an anechoic chamber must provide a truly free space test environment. The performance of a rectangular RF anechoic chamber can be determined by measuring the relative insertion loss versus separation distance between a source antenna and a receiving antenna.

Antenna insertion loss is the ratio of power received by a receiving antenna or probe to the power accepted by the transmitting antenna. If the anechoic chamber is a perfect free-space simulator, the relative insertion loss between two polarization-matched antennas will vary with distance according to the Friis transmission formula (9)

$$P_r/P_t = G_r G_t (\lambda/4\pi d)^2 \quad (39)$$

where  $P_t$  is the net power delivered to the transmitting antenna,  $P_r$  is the power received by the receiving antenna,  $G_t$  is the near-field gain of the transmitting antenna,  $G_r$  is the near-field gain of the receiving antenna,  $d$  is the separation distance between the two antennas, and  $\lambda$  is the wavelength. Experimental data can be compared with the calculated free space transmission loss, using appropriate near-field transmitting antenna gains. The difference between the measured and calculated transmission loss is a measure of reflections from chamber surfaces.

### Open Area Test Sites

An open area test site typically is used for the antenna calibration in the frequency range of 10 kHz to 1000 MHz. A calibration consists of determining the antenna factor that permits a receiver (RF voltmeter) to be used with the calibrated antenna to conduct measurements of field strength.

At frequencies below about 50 MHz, loop antennas are calibrated in a quasi-static, near-zone, magnetic field produced by a balanced single turn transmitting loop with a 10 cm radius. Above 25 MHz, dipole antennas are calibrated in a far-zone electric field, which is evaluated in terms of the open circuit voltage induced in a self-resonant receiving dipole antenna. Between 30 kHz and 300 MHz, vertical monopole antennas and small probes are evaluated in an elliptically polarized electromagnetic field produced by a transmitting monopole antenna above a conducting ground screen.

Field strength can be evaluated using two independent techniques: (1) the standard field method, and (2) the standard antenna method. For the standard field method, a transmitted field is calculated in terms of the type and dimensions of a transmitting antenna, its current distribution or net de-



livered power, the frequency of the transmitted signal, the distance from the transmitting antenna to the field point, and the effect of ground reflections (if present). For the standard antenna method, an unknown field is measured with a calculable receiving antenna. The voltage or current induced in a standard antenna by the component of field being evaluated is measured. The field strength then is calculated in terms of this induced voltage, the dimensions and form of the receiving antenna, and its orientation with respect to the field vector.

All of the techniques described above for field strength standards are applicable only to steady state RF fields with sinusoidal time variation. They are not intended for use with pulsed fields or other broadband applications.

#### Magnetic Field Strength Standards for Loop Antennas at 10 kHz to 50 MHz (Standard Field Method)

The response of an electrically small receiving loop antenna is proportional to the average normal component of magnetic field strength incident on the antenna. A calculable quasi-static magnetic field can be produced to calibrate these antennas using a circular single-turn balanced transmitting loop. Up to 30 MHz, the current in a loop with a 10 cm radius is approximately constant in amplitude and phase around the loop. The receiving loop antenna being calibrated is positioned on the same axis as the transmitting loop at a distance of 1.5 m to 3 m. The normal component of the magnetic field, averaged over the area of the receiving loop, is given by (10)

$$H = \frac{\beta I r_1}{r_2} \sum_{m=0}^{\infty} \frac{1}{(2m+1)!} \cdot \frac{1 \cdot 3 \dots (2m+1)}{2 \cdot 4 \dots (2m+2)} \left[ \frac{\beta r_1 r_2}{R_0} \right]^{m+1} h_{2m+1}^{(2)}(\beta R_0) \quad (40)$$

where

- $H$  = rms value of the magnetic field
- $I$  = rms current in the transmitting loop
- $r_1$  = radius of the transmitting loop
- $r_2$  = radius of the receiving loop
- $R_0 = \sqrt{d^2 + r_1^2 + r_2^2}$
- $d$  = axial distance between the two loops
- $\beta = 2\pi/\lambda_0$
- $\lambda_0$  = free-space wavelength
- $h_n^{(2)}$  = nth order spherical Hankel function of the second kind

The current in the transmitting loop antenna is measured with a vacuum thermocouple calibrated with direct current. The thermocouple is at the top of the loop winding.

While coaxial loop antennas normally are used for calibration purposes, the two loop antennas also can be positioned in the same plane. Coplanar loop antennas are advantageous under certain conditions (e.g., with some ferrite core antennas in which the core length is large). In the coplanar loop antenna set-up, the calibrating value of  $H$  would be half of that given by Eq. (41).

The calibration and subsequent measurement of magnetic field strength  $H$  often are expressed in terms of the electric field  $E$  that would exist if the measurement were made in free space, in which case  $E/H \cong 120\pi \Omega$ . When such a field strength meter is used to make measurements near the ground, the indicated value of the electric field is not necessarily valid. The same is true for measurements made in the

near zone of a transmitting antenna. However, the value of the magnetic component  $H$  still can be measured correctly.

For calibrating loop antennas or magnetic field sensors at a higher field, it is possible to use the calculable magnetic field generated in a TEM cell, or a waveguide chamber, or at the center of a flat multiturn coil, or at the midpoint of a Helmholtz coil pair.

#### Electric Field Strength Standards for Dipole Antennas from 25 MHz to 1000 MHz (Standard Antenna Method)

The magnitude of the electric field component at a given point in a locally generated field is determined from the open circuit voltage  $V_{oc}$  induced in a standard (calculable) half-wave receiving dipole antenna. The induced voltage is measured across the center gap of the dipole antenna, which is oriented parallel to the electric field vector of the incident field. In using the standard antenna method, a plane wave field can be generated by a suitable transmitting antenna, such as a log periodic or half-wave dipole antenna. The magnitude of this incident field is measured with the standard dipole antenna by the relation

$$E_{inc} = \frac{V_{oc}}{L_{eff}} \quad (41)$$

where  $E_{inc}$  is the field strength of the locally generated field,  $V_{oc}$  is the open circuit voltage induced in the standard dipole antenna, and  $L_{eff}$  is the effective length of the standard dipole antenna.

The RF voltage  $V_{oc}$  picked up by the  $\lambda/2$  standard dipole is detected by a high-impedance Schottky barrier diode connected in shunt across the center gap of the antenna. The diode output is filtered by a balanced  $RC$  network, and this dc voltage is measured with a high-impedance dc voltmeter. The RF-to-dc characteristic of the dipole antenna and its filter circuit is obtained experimentally. Assuming a cosinusoidal current distribution on an infinitesimally thin dipole, the effective length of a half-wave dipole antenna in free space is given by Eq. (12).

#### Electric Field Strength Standards for Vertical Monopole Antennas 30 kHz to 300 MHz (Standard Field Method)

Several approaches were considered for generating a standard (calculable) field to calibrate vertically polarized antennas. The system chosen for this measurement consists of a thin cylindrical transmitting monopole antenna over a metallic ground plane. The field strength is calculated in terms of the magnitude and distribution of the monopole antenna current, and other factors such as: (1) monopole height, (2) horizontal distance from the transmitting antenna to the field point, (3) vertical height of this point above the ground plane, and (4) electrical conductivity of the ground plane.

The height of the transmitting monopole antenna is adjustable, with a maximum height of about 3 m. The electrical height of this antenna is  $\lambda/4$  (resonant) at 25 MHz, but only  $0.0003 \lambda$  at 30 kHz. At frequencies above 25 MHz, the antenna height is reduced to a  $\lambda/4$  value. The base diameter of the monopole antenna is about 1 cm. The monopole antenna is excited through a coaxial cable from a transmitting room located beneath a concrete ground slab which is covered by a conducting metal screen to form the electrical ground plane.

Equations (42), (43), and (44) give the magnitudes of the three field components  $E_z$ ,  $E_\rho$ , and  $H_\phi$ , respectively, of a transmitting  $\lambda/4$  monopole antenna above a perfect ground plane of infinite extent:

$$E_z = 30I_0 \left( \frac{e^{-j\beta r_1}}{r_1} + \frac{e^{-j\beta r_2}}{r_2} \right) \quad (42)$$

$$E_\rho = \frac{30I_0}{r_0} \left[ \left( \frac{e^{-j\beta r_1}}{r_1} \right) \left( z - \frac{\lambda}{4} \right) + \left( \frac{e^{-j\beta r_2}}{r_2} \right) \left( z + \frac{\lambda}{4} \right) \right] \quad (43)$$

$$H_\phi = \frac{I_0}{4\pi r_0} (e^{-j\beta r_1} + e^{-j\beta r_2}) \quad (44)$$

where

- $E_z$  = vertical electric field component
- $E_\rho$  = horizontal electric field component
- $H_\phi$  = magnetic field, encircling the monopole antenna
- $I_0$  = rms base current of the monopole antenna
- $\beta = 2\pi/\lambda$  = the wavelength constant
- $r_1 = [d^2 + (z - l)^2]^{1/2}$
- $r_2 = [d^2 + (z + l)^2]^{1/2}$
- $r_0 = [d^2 + z^2]^{1/2}$
- $l$  = monopole antenna length
- $d$  = horizontal distance between the monopole antenna and the field point
- $z$  = vertical distance from the ground plane to the field point

For frequencies near self-resonance, the monopole antenna base current is measured with an RF ammeter consisting of a thermo-converter that has been calibrated with known values of dc current. At lower frequencies, where the monopole antenna input impedance  $Z_{in}$  is a high-capacitive reactance, the base current is calculated from Ohm's law in terms of the base voltage measured with a high-input impedance voltmeter and the theoretical input impedance. At very low frequencies,  $Z_{in}$  may be calculated from the antenna capacitive reactance (11).

$$Z_{in} = 1/(j\omega C_a) \quad (45)$$

where

$$C_a = \frac{5.56 \times 10^{-11} h}{\ln(h/a) - 1} \quad (46)$$

where  $C_a$  is the monopole antenna input capacitance (F),  $h$  is the monopole antenna height (m), and  $a$  is the monopole antenna radius (m).

The standard field equations are relatively simple for a ground plane with infinite extent and infinite conductivity. In addition, the current on a vertical monopole antenna with finite diameter departs from the sinusoidal current distribution of a filamentary monopole antenna. This does not seriously affect the calculated values of current-related field components, such as the magnetic field or the far-zone electric field. However, the low-frequency near-zone quasi-static electric field components are more nearly charge-related and are given by the spatial derivative of the current distribution. Hence, there is greater uncertainty in calculating the electric field components at frequencies well below that of a  $\lambda/4$ -resonant monopole antenna.

If a transmitting monopole antenna is electrically short; that is, if the height is less than  $\lambda/4$  and the frequency is below resonance, the current distribution is triangular. The field equations are a little more complicated; only the vertical electric field is given below (11)

$$E_z = \frac{-j30I_0}{\sin(\beta\ell)} \left[ \frac{e^{-j\beta r_1}}{r_1} + \frac{e^{-j\beta r_2}}{r_2} - 2 \cos(\beta\ell) e^{-j\beta r_0} \right] \quad (47)$$

The EM field values in the half space above a perfect ground are the same as those in each half volume of a center fed  $\lambda/2$  dipole antenna in free space. The input impedance of a monopole antenna above perfect ground is half that of a dipole antenna in free space. The power required to generate a given field strength is half that required for a dipole antenna, but the radiated power goes into half the volume, so the field is the same. Measurements of  $Z_{in}$  with a commercial impedance meter are performed to check the theoretical values from 0.5 MHz to 50 MHz. Measurements of the monopole antenna capacitance can be made at lower frequencies with a commercial  $Q$  meter.

## FUTURE DIRECTIONS

Established techniques for EM field measurements will be probably extended to higher frequencies; however, such work would not involve fundamental changes in the instrumentation or measurement strategy. The measurement methods described earlier are suitable only for (1) measuring plane-wave sinusoidal fields of a given frequency and (2) calibrating the devices that measure such fields.

The challenge of the future resides in the development of standards for measurement of fields that are nonsinusoidal and/or nonplanar. The fundamental requirement for EM field sensors is that their outputs provide amplitude and phase information simultaneously over a broad spectrum for nonsinusoidal fields. For fields containing more than one frequency component, it is clear that such simultaneous measurement is necessary. Similarly, if phase information is preserved, then measurements of single-frequency nonplanar fields can be made in terms of true energy density or in terms of the Poynting vector.

The standard techniques of today rely upon very high-resistance transmission lines to convey dc voltage and current to regions external to the field under measurement. Future standards of measurement employ optically sensed EM field sensors whose optical-sensing signal paths will not perturb the EM field under measurement, but will also convey field amplitude and phase information to a region external to the field for measurement. Optically sensed sensors are being built today. However, additional work is needed to transform these experimental devices into stable elements for standards applications. Also, standard fields need to be developed, in order to calibrate these probes of the future.

## BIBLIOGRAPHY

1. M. Kanda, Standard probes for electromagnetic field measurement, *IEEE Trans. Antennas Propag.*, **AP-41**: 1349–1363, 1993.
2. M. Kanda, Analytical and numerical techniques for analyzing an electrically short dipole with a nonlinear load, *IEEE Trans. Antennas Propag.*, **AP-28**: 71–78, 1980.

3. M. Kanda, A relatively short cylindrical broadband antenna with tapered resistive loading for picosecond pulse measurements, *IEEE Trans. Antennas Propag.*, **AP-26**: 439–447, 1978.
4. M. Kanda and L. D. Driver, An isotropic electric-field probe with tapered resistive dipoles for broadband use, 100 kHz to 18 GHz, *IEEE Trans. Microw. Theory Tech.*, **MTT-35**: 124–130, 1987.
5. M. Kanda, An electromagnetic near-field sensor for simultaneous electric and magnetic field measurements, *IEEE Trans. Electromagn. Compat.*, **EMC-26**: 102–110, 1984.
6. L. D. Driver and M. Kanda, An optically linked electric and magnetic field sensor for Poynting vector measurements in the near fields of a radiating source, *IEEE Trans. Electromagn. Compat.*, **30**: 495–503, 1988.
7. M. Kanda and K. D. Masterson, Optically sensed EM-field probes for pulsed fields, *Proc. IEEE*, **80**: 209–215, 1992.
8. J. C. Tippet, *Model characteristics of rectangular coaxial transmission line*, Ph.D. Dissertation, E.E. Department, University of Colorado, Boulder, 1978.
9. S. A. Schelkunoff and H. T. Friis, *Antennas, Theory and Practice*, New York: Wiley, 1952.
10. F. M. Greene, The near-zone magnetic field of a small circular-loop antenna, *J. Res. Nat. Bur. Stand. U.S. C. Eng. and Instr.*, **71C** (4): 1967.
11. E. C. Jordan and K. G. Balmain, *Electromagnetic Waves and Radiating Systems*, Englewood Cliffs, NJ: Prentice-Hall, 1968.

MOTOHISA KANDA  
National Institute of Standards and  
Technology

**ELECTROMAGNETIC FIELDS.** See RADAR REMOTE SENSING OF IRREGULAR STRATIFIED MEDIA.

**ELECTROMAGNETIC FIELDS, BIOLOGICAL EFFECTS.** See BIOLOGICAL EFFECTS OF ELECTROMAGNETIC FIELDS.

**ELECTROMAGNETIC FIELD THEORY.** See BOUNDARY-VALUE PROBLEMS.